

Do Green Infrastructure Types Represent Land Surface Temperature? A Case Study of Stuttgart

Alejandra Narváez Vallejo^{1,2}, Hans-Georg Schwarz-v.Raumer¹

¹University of Stuttgart, Stuttgart/Germany · svr@ilpoe.uni-stuttgart.de

²Municipality of Stuttgart, Dept. of Geoinformation and Cartography/Germany

Abstract: To combat urban heat islands, comprehensive data on how urban morphological configuration affects temperature is needed. Remote sensing offers diverse products to characterize land surface and to monitor its character, and evaluate changing urban structure typologies. Green Infrastructure Typology (GIT) by Bartesaghi-Koc et al. (2019) is a relatively new typology that combines physical structure (vegetation strata, built structures and water) and spatial descriptors of urban structures as a basis to describe urban climate parameters. Using the city of Stuttgart, Germany as a case study, we assessed the land surface temperature (LST) of GIT classes. Our results indicate that GIT can be adapted for Stuttgart and be used as an approximation to identify urban heat islands and cooler areas, making it a valuable tool for planning resilient and sustainable cities.

Keywords: Land surface temperature, Green Infrastructure Typology, urban morphology, urban heat mitigation.

1 Introduction

Increasingly, people are moving from rural areas to urban centres leading to the densification of cities and competition for space. These processes modify the landscape structure as natural cover is replaced with artificial surfaces, thereby altering ventilation and modifying the heat balance (SANTAMARIOUS 2015). Such changes, in combination with Global Climate Change (GCC), lead to warming cities and can dangerously affect human well-being (NGARAMBE et al. 2022). Urban heat mitigation is a key issue for governments, scientists and planners worldwide (MOHAMMED et al. 2022). An important strategy for urban heat mitigation is to foster urban resilience and sustainable development with Green Infrastructure elements such as parks, lawns, trees, green roofs, green facades, and their effective inclusion into the urban matrix.

Vegetation reduces land surface temperature (LST) through shading, advection and evapotranspiration, and mitigates the surface urban heat island (SANTAMOURIS 2015). Satellite-based remote sensing LST products have helped monitor and investigate micro-urban heat islands and their relationship with vegetation cover for at least two decades (ANIELLO et al. 1995, KAPLAN et al. 2018, RANAGALAGE et al. 2017). Today, such data is easily available and accessible with global coverage and high temporal resolution (e. g. 16 days for Landsat).

Assessment of the thermal benefits of urban vegetation, which is embedded in a complex and heterogeneous environment, requires a holistic analysis that considers the different types of vegetation strata, land cover proportion and spatial arrangements, as well as human-meteorological effects. Structural typologies of urban land surfaces help to translate urban and human-meteorological complexity into planning suggestions. With this aim, many typologies and protocols have been proposed, such as the Local Climates Zones (LCZ) by STEWART &

OKE (2012), the High Ecological Resolution Classification for Urban Landscapes and Environmental Systems (HERCULES) suggested by CADENASSO et al. (2007), the Urban Vegetation Structure Types (UVST) introduced by LEHMANN et al. (2014) and more recently the "Green Infrastructure Typology (GIT)"¹ by BARTESAGHI-KOC et al. (2019a). GIT, though conceptually similar to the other approaches mentioned, is constructed with simpler landscape metrics and is easier to apply across multiple spatial scales.

GIT was essentially formulated for climate aspects, but can also support other performance-based analyses across different ecosystem services. Various studies on Sydney, Australia, have successfully evaluated and compared the intra- and inter-type variability of land surface temperatures (LST) (BARTESAGHI-KOC et al. 2019a). These studies have demonstrated its capacity for fast identification of hotspots to prioritise urban areas for heat mitigation (BARTESAGHI-KOC et al. 2019b) and have assessed the thermal seasonal behaviour of urban landscape configurations (BARTESAGHI-KOC et al. 2020).

Motivated by its simplicity, integral vegetation-oriented approach and the positive results of previous climate-oriented studies, we adapted and applied the GIT approach for Stuttgart and evaluated the thermal behaviour of its types. The current study aims to answer the following questions: (a) Is GIT capable of catching the urban structural variability of Stuttgart? (b) Does GIT reflect land surface temperature (LST) differences as a basis for indicating heat stress and heat relaxation? and (c) Does the applied size of the spatial units for applying the typology matter?. We hypothesize that an analysis of GIT is a good predictor of LST. We test that by applying a simple statistical analysis of spatial coincidence.

2 Detection of Vegetation Structures

It seems simple, but a comprehensive inventory of urban vegetation structures requires the complex merging of data sets that are built up and maintained with very different intentions. Three of the most fundamental datasets are: (1) green space, tree and forest cadastres, (2) biotope mappings and (3) surveys of roof and facade greening.

In the context of blue-green infrastructure, vegetation structures are considered in terms of the preservation of the vitality of vegetation under climate change conditions. Here, details of vegetation structures and the requirement to have a citywide inventory play an important role, and there is a need for information on vegetation composition and height. Green volume and leaf area index have become urban GCC adaption quality assessment indicators (VOLK et al. 2022). Both provide a basis for a rough assessment of the temperature-regulating evapotranspiration capacity of the vegetation. As a pragmatic solution in a large-scale study, the combination of height and growth form or morphology types (e. g., arboreal, shrub, perennial, perennial vegetation, turf) are considered sufficient indicators.. However, the more we address the climate-vegetation relation on a local scale, the more detailed and species-specific the characterisation of the plant communities should be.

As a part of the project "Integrated strategies to strengthen blue-green infrastructures (INTERESS-I)" (<https://www.interest-i.net/>), object-based image classification methods (e. g. PLATT & RAPOZA 2008) were used to detect vegetation objects at very high spatial

¹ We use the term "green infrastructure typology" directly as it is used by BARTESAGHI-KOC et al. (2019a) without discussing its proper use.

resolution (0.5 m) using both spectral and structural data. The spectral information refers to 0.5 m resolution Pleiades-I images from the 10th and 16th of May 2017, acquired as an ESA's Third-Party Mission within the ESA TPM project research ID 49634. The structural data were extracted from Light Detection And Ranging (LIDAR) data captured in 2016 (average first return point density 16.6 pts/m²) and provided by the Landesamt für Geoinformation und Landentwicklung, Baden-Württemberg (LGL). The classification and preprocessing of the data was carried out using the software eCognition developer 10.0. Due to missing data, only 89 % of the city area could be classified, covering 184 km² (hereinafter referred to as study area, shown in Figure 1).

Seven land cover types were separated at a high level of accuracy²: water, no vegetation (i. e. buildings, streets, bare soil) and five vegetation classes that include three ground vegetation classes – grass or low (≤ 1 m), bushes or medium (1 m – 2.5 m) and trees or high (>2.5 m) – and two roof vegetation classes – grass or low (≤ 1 m) and bushes/trees (>1 m) (Figure 1).

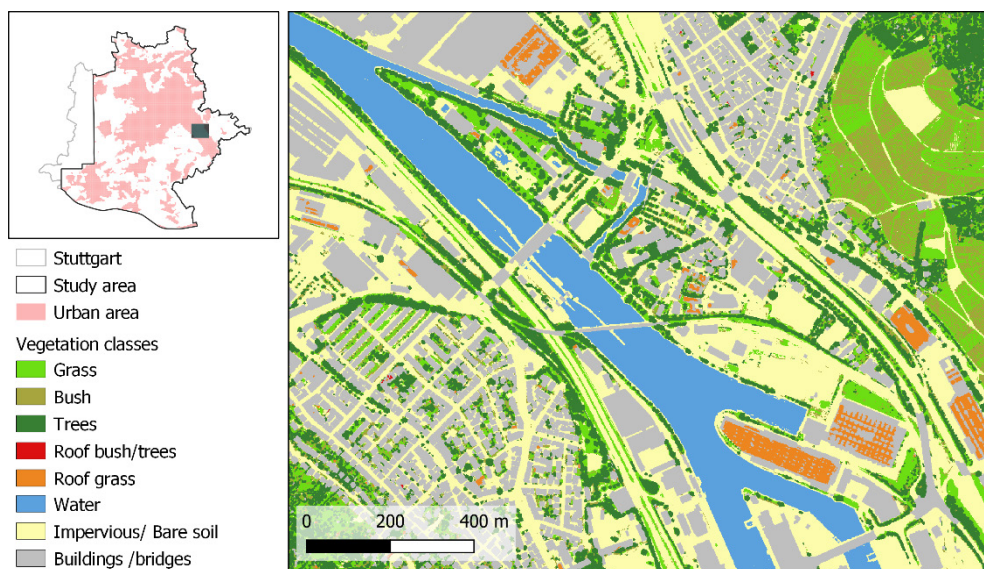


Fig. 1: Example for the classification results. ‘Urban area’ refers to the complete study area excluding forest and agricultural land > 4 ha

² For the ground cover classes, the user accuracies per class (probability that a particular location the class is classified correctly) were at least 0.90, and the overall accuracy (proportion of correctly classified reference sites) for the images were approximately 96 %. The roof classes were validated based on the capacity to detect the vegetation on roofs units, the sensitivity (probability that a detected vegetated roof is vegetated) and the specificity (probability that detected non-vegetated roof is non-vegetated as well) exceed 0.84.

3 Land Surface Temperature: Identifying Heat Spots and Cooling Islands

Urban heat island (UHI) is defined as an urban built-up area that is significantly warmer than its surrounding rural countryside due to anthropogenic activities. This can be studied by two closely coupled phenomena: the surface urban heat island (SUHI) and the meteorological (atmospheric) urban heat island (PHELAN et al. 2015). In particular, SUHI is governed by local aspects that depend on the physical properties of natural and man-made materials constituting the urban morphology (BARTESAGHI-KOC et al. 2020).

LST as a spatially distributed measurement is used to assess SUHI. It captures the differential thermal behaviour of surface materials. Built-up structures, roads and other sealed surfaces store heat and accentuate heat islands, while vegetation and water surfaces promote cooling effects through evapotranspiration, shading and modification of heat exchange through advection (SANTAMOURIS 2015). Therefore, a thematic map of LST indicates the location of warmer or cooler areas and should be included in all urban meteorological planning records.

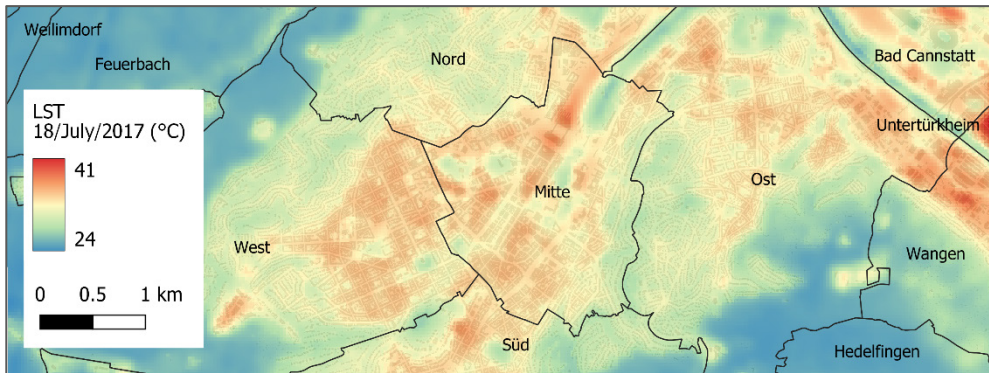


Fig. 2: Land surface thermal map, centre of Stuttgart City

The LST data for our study area were obtained from validated products provided by Landsat 8 (<https://earthexplorer.usgs.gov/collection/2/level/2>). The images were acquired on 18 of July 2017 around 10am and delivered at 30 m resolution. They were scaled to Kelvin using the scaling factors of the product and then rescaled to degrees Celsius (USGS 2022). The original rasters were cropped to the study area and clouds were masked out (one small one). LST was then aggregated by the mean to raster layers at 60 m and 90 m resolution.

4 Area Typing: Morphology Makes Climate

4.1 GIT Basics in a Nutshell

The Green Infrastructure Typology (GIT) from BARTESAGHI-KOC et al. (2019a) is a holistic approach overarching principles of multi-functionality, connectivity and dynamic spatio-temporal heterogeneity (BARTESAGHI-KOC et al. 2020). The scheme comprises 34 standard

Green Infrastructure Types (GI_t, plural: GI_{ts}), each defined by a unique combination of physical characteristics of land surface (proportion and composition of surfaces: water, imperious, grass, bush and trees) and spatial descriptors of tree patterns (patch elongation, CIRCLE_AM³; and patch clumpiness, nLSI⁴ as described in MCGARIGAL (2015)). Each of the GI_{ts} is assigned to one of the following broad groups: a) '*Impervious* areas with a high proportion of sealed surfaces and/or buildings', b) '*Mixed* areas comprising a variety of biotic and abiotic infrastructure', c) '*Pervious*, natural areas with minimal anthropogenic structures' and d) '*Aquatic* areas with a significant proportion of water bodies'.

If the typing is available as a spatial assignment to units like cells in a regular grid, human-meteorological parameters, such as the cooling effect, can be spatially assigned to the units at a rank scale (BARTESAGHI-KOC et al. 2020). Therefore, GIT can guide GCC-adaption measures, the restructuring of urban morphology or climate-adapted urban development.

4.2 Implementing GIT in Stuttgart City

We divided the study area (see Figure 1) into grid cells at 30 m (division is abbreviated as 30G), 60 m (60G) and 90 m (90G) resolution to calculate the metrics and assign the GI_{ts}. For the implementation of GIT in Stuttgart, three changes needed to be introduced.

First, the original GIT distinguishes between irrigated and non-irrigated grasses, while our classification does not – there is only grass (details in Table 1).

Second, the GIT for the study area also includes roof greening, which like the ground vegetation has cooling effects (ASADI et al. 2020). Low roof vegetation was considered as grass and higher roof vegetation as trees.

Third, the original GIT, though effectively classifying around 98% of the study area, fails to classify around 400 ha in the core urban area. After a careful inspection of the unclassified areas, two important adoptions were implemented: (1) The upper limit of the trees percentage of classes IM4c, IM5c, IM6c was increased by 10 %, MX2c, AQ4c by 15 % and MX5c by 25 %, while ensuring the main characteristics of the GI_{ts} were maintained. (2) River Neckar port was introduced as a type called "highly impervious with water" (HA). The adoptions lead to a decline of unclassified land to less than 0.3 %.

Finally, we applied a GIT consisting of 30 GI_{ts} (Tab. 1). Figure 3 shows the GI_{ts} percentage occurring in the study area and the mean distribution of land covers per GI_t at 60G. These results are very similar for the 30G and 90G divisions.

5 Characterising Land Surface Temperatures of GI_{ts}

The characterisation of the GI_{ts} by LST focuses on cooling effects and on whether grid resolution plays a role. These questions were targeted specifically for the urban area, thus all forest and agricultural areas greater than 4 ha were excluded from the analysis (Fig. 1).

³ Related circumscribing circle- area weighted.

⁴ Normalized landscape shape index.

Table 1: Parameters and threshold values for the adapted GIT classification. On parenthesis BARTESAGHI-KOC (2019) thresholds. * Impervious class also comprises bare soil; for further comparison refer to BARTESAGHI-KOC et al. (2019a)

GIT	Description	Surface fractions of cell area (%)						Trees Sp. Config.	
		*Impervious	Grass	Shrubs	Trees	Water	Circle_AM	mLSI	
Impervious	IM1	Highly impervious	≤ 25	≤ 25	≤ 25	≤ 25	≤ 25		
	IM2	Mostly impervious with grasses	>50 ≤ 75	< 50	≤ 25	≤ 5	≤ 25		
	IM3	Mostly impervious with shrubs	>25 ≤ 75	< 40	>25 ≤ 50	≤ 25	≤ 25		
	IM4c	Mostly impervious with aligned trees	>50 ≤ 75	< 40	≤ 25	>5 ≤ 50 (40)	≤ 25	∧ 0,61	< 0,25
	IM5c	Mostly impervious with scattered trees	>50 ≤ 75	< 40	≤ 25	>5 ≤ 35 (25)	≤ 25	< 0,61	> 0,065
	IM6c	Mostly impervious with clustered trees	>50 ≤ 75	< 40	≤ 25	>5 ≤ 50(40)	≤ 25	< 0,61	> 0,065
Mixed	MX2c	Mostly grasses with impervious	>25 ≤ 50	> 50	≤ 25	≤ 20 (5)	≤ 25		
	MX3	Mixed surfaces without trees	>25 ≤ 50	< 75	≤ 25	≤ 5	≤ 25		
	MX4	Mixed grasses and bare soils	>25 ≤ 50	< 75	≤ 25	≤ 5	≤ 25		
	MX5c	Mixed surfaces with aligned trees	>25 ≤ 50	< 50	≤ 25	>5 ≤ 75(50)	≤ 25	∧ 0,61	< 0,25
	MX6	Mixed surfaces with aligned trees	≤ 25	< 50	≤ 25	>5 ≤ 75	≤ 25	∧ 0,61	< 0,25
	MX7	Mixed surfaces with scattered trees	>25 ≤ 50	< 50	≤ 25	>5 ≤ 50	≤ 25	< 0,61	> 0,065
	MX8	Mixed grasses with scattered trees	≤ 25	< 50	≤ 25	>5 ≤ 75	≤ 25	< 0,61	> 0,065
	MX9	Mixed surfaces with clustered trees	>25 ≤ 50	< 50	≤ 25	>5 ≤ 75	≤ 25	< 0,61	> 0,065
	MX10	Mixed grasses with clustered trees	≤ 25	< 50	≤ 25	>5 ≤ 75	≤ 25	< 0,61	> 0,065
	PV2c	Mostly grasses	≤ 25	> 75	≤ 25	≤ 5	≤ 25		
Pervious	PV3	Mixed grasses with shrubs and trees	≤ 25	< 60	≤ 50	≤ 50	≤ 25		
	PV4	Mostly shrubs	≤ 25	< 50	> 50	≤ 25	≤ 25		
	PV6	Mostly grasses with aligned trees	≤ 25	> 50	≤ 25	>5 ≤ 50	≤ 25	∧ 0,61	< 0,25
	PV8c	Mostly grasses with scattered trees	≤ 25	> 50	≤ 25	>5 ≤ 50	≤ 25	< 0,61	> 0,065
	PV10c	Mostly grasses with clustered trees	≤ 25	> 50	≤ 25	>5 ≤ 50	≤ 25	< 0,61	> 0,065
	PV11	Dense trees with shrubs and grasses	≤ 25	< 25	≤ 75	> 75	≤ 25	< 0,61	> 0,065
Aquatic	AQ1	Water	≤ 25	< 25	≤ 25	≤ 25	> 75	∧ 75	
	AQ2	Mostly water with grasses	≤ 25	< 40	≤ 25	≤ 5	>50 ≤ 75		
	AQ3	Mostly grasses with water	≤ 25	< 60	≤ 25	≤ 5	>25 ≤ 50		
	AQ4c	Mixed surfaces with water	>25 ≤ 50	< 50	≤ 25	> 40(25)	>25 ≤ 75		
	AQ5	Water with aligned trees	≤ 25	< 40	≤ 25	>5 ≤ 75	>25 ≤ 75	∧ 0,61	
	AQ6	Water with scattered trees	≤ 25	< 40	≤ 25	>5 ≤ 40	>25 ≤ 75	< 0,61	
	AQ7	Water with clustered trees	≤ 25	< 40	≤ 25	> 40	>25 ≤ 75	< 0,61	
HA	Hafen: Highly impervious with water	>50 ≤ 75	< 50	≤ 25	≤ 25	>25 ≤ 50			

The total assessed area was 95 km², 88 km² and 82 km² for 30G, 60G and 90G respectively. Only the GITs represented by at least five samples were taken into account for this analysis.

The cooling effect (Ceff) of each GIT was calculated as its median temperature (mGIT) minus the median temperature of the highly impervious GIT (mIM1):

$$C_{eff} = mGIT - mIM1 \tag{Eq. 1}$$

By comparing the LST of the different GITs, it becomes evident that temperature levels of the main groups vary from warmest to coldest according to the sequence: impervious-mixed-pervious-aquatic (Fig. 3).

Inspired by the study conducted by ZHOU et al. (2011), we hypothesised that the resolution of the grid cell size chosen for analysis influences the result. Our results show that the temperature difference between some types becomes much more evident in the 60G and 90G than in 30G division (for example MX10, PV2, PV3) (Fig. 4). Similarly, the results indicate that though in 30G Ceffs of the different GITs can be detected, this is less pronounced than on larger grid sizes (Fig. 5). Additionally, the data dispersion and the number of extreme values reduce with increasing grid size (Fig. 5). All these findings are in line with ZHOU et al. (2011) who argue that much of LST variance is explained at coarse resolution by land cover composition, while more factors need to be considered to understand the behaviour of LST at finer scales.

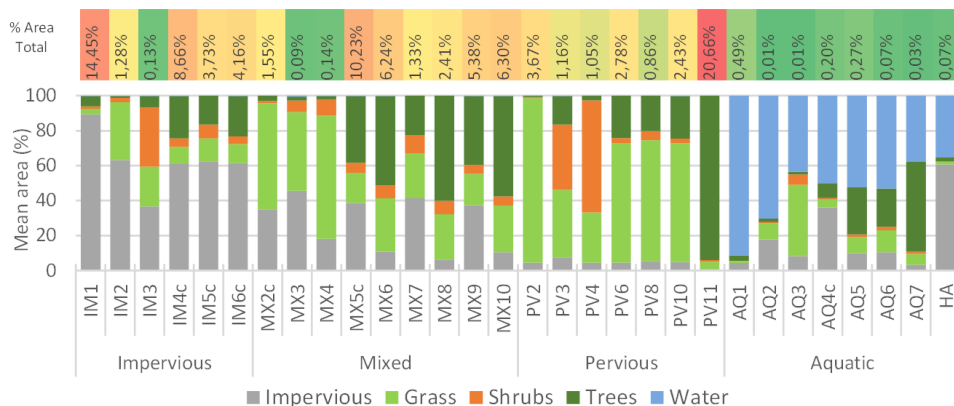


Fig. 3: GITs percentage of the total study area and mean distribution of land covers for each GITs at 60G

Figure 5 allows for the identification of differences among the cooling capacities of the GITs. Within the *impervious* types, the GITs with the largest percentage of tree cover (IM4c, IM5c, IM6c) consistently reveal a cooling effect of approximately 2 °C. Similarly, IM3, with the overall highest percentage of vegetation in the group, reached 1.9 °C cooling at 30G.

In general, the aquatic group presented the highest cooling capacity. The maximum cooling capacity is located in AQ1, reaching Ceff = 9.6 °C in 90G. Next, the tree-dominated GITs show Ceff between 5.6 °C and 8.4 °C. The remaining GITs of the group have lower Ceffs in accordance with the increase in impervious cover and decrease in tree cover.

In the *mixed* GIs, three groups can be identified: GIs with (a) *minor* cooling capacity (Ceff between 0 °C and 2.6 °C) having low tree cover (average below 3 %) comprising MX2c, MX3, MX4, GIs with (b) *significant* cooling capacity (Ceff between 2,7 °C and 4,1 °C) having medium tree cover (average 20 % to 40 %) and a medium percentage of impervious area (approx. 40 %) consisting of MX5c, MX7, MX9 and GIs with an (c) *extraordinary* cooling capacity (Ceff between 3,9 °C and 6,5 °C) having high tree cover (average above 50 %) and a low percentage of impervious surface (average below 26 %) including MX6, MX8, MX10.

In the *pervious* group, PV11 shows the highest cooling capacity in all resolutions, reaching Ceff = 8.2 °C at 90G. As in the other main groups, the Ceff of the GIs with more tree cover (PV6, PV8, PV10) are the highest, averaging a Ceff of 5.1°C. Nevertheless, PV2 (mostly grasses) and PV3 (mostly grasses and bushes) also achieve Ceff up to 4.6°C. PV4, associated mostly with urban vineyards, showed an astonishingly low cooling effect. This affect is attributed to the sun exposition of the terrain. In Germany, grapes are mainly cultivated on south-facing slopes to obtain the most sunlight and heat. As a result, the topographic position of PV4 makes it warmer and masks the cooling effect of vegetation.

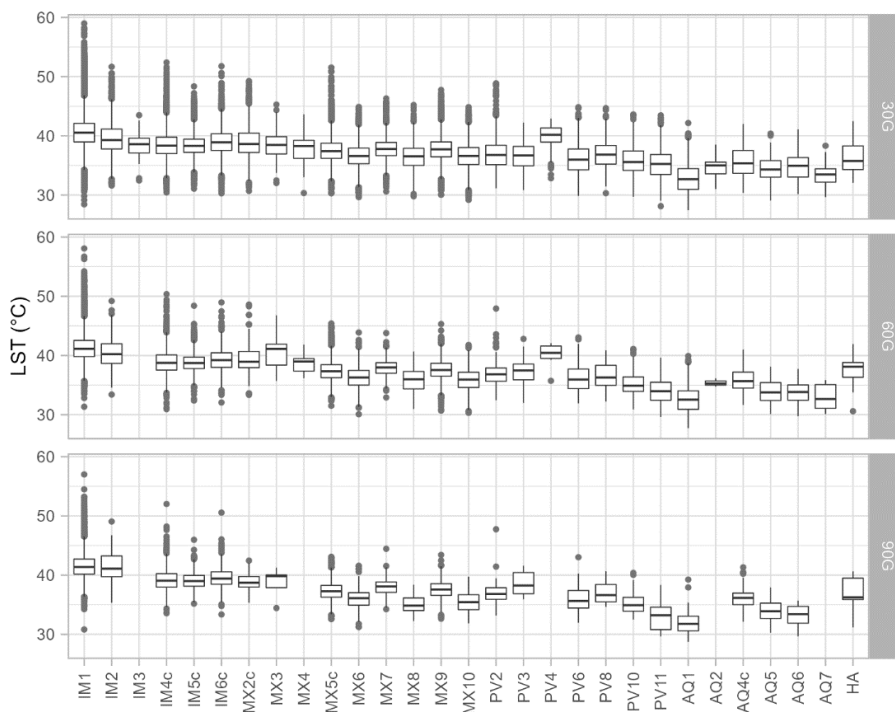


Fig. 4: LST distribution as Boxplot of each GI for the different resolutions

The results show clear differences in the cooling capacity of the GIs driven mostly by their land cover composition. In general, the high cooling capacity of areas with significant tree cover indicates that this vegetation type is the most important for urban cooling as indicated

in other studies (ZAIN ET AL. 2015). Besides trees and water surfaces, considerable cooling effects was achieved by large extensions of other vegetation covers. However, such configurations are rare in urban development plans due to high competition for space.

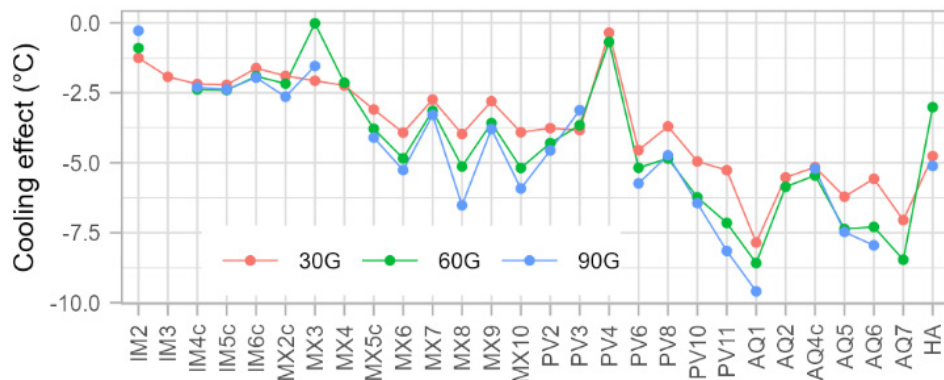


Fig. 5: Cooling effect of the GITs at different resolutions

6 Conclusions and Recommendations

Our study shows that GIT is a good predictor of LST and can be used as a proxy to urban heat island detection.

The study shows that the Stuttgart consists of a big range of various GITs. The applied GIT sufficiently typecasted structural arrangements and morphologies that are common in European cities such as Stuttgart, Germany. It's simple approach allows for adaptations like the incorporation of previously unclassified classes (e. g. river port type) or the extension of class thresholds.

Regarding GIT implementation, attention must be paid when selecting the resolution for analysis. In the case of LST analysis, the thermal effects are stressed at larger evaluation units, but there is a higher risk that some GITs will not be represented.

Using GIT in conjunction with free satellite products such as Landsat is an excellent option for evaluating the thermal behaviour of urban arrangements. Moreover, these images' regular availability could be used to track GITs throughout the year and for several time intervals. This would allow for the assessment of changes in their thermal characteristics, which is important since vegetation is a living and dynamic component of urban structures.

Our results confirm that trees and water surfaces have considerable cooling effects. This can also be achieved with large areas of other vegetation cover, however, such configurations are not the most desirable in city planning due to the high competition for urban space.

Although topographic effects on the characterisation of GITs in terms of LST were not evaluated, the results suggest that sun exposition is a relevant factor. We therefore suggest that future studies carry out LST analyses of GITs using a stratification according to topographic variables (aspect, slope, elevation). Such studies could not only indicate favorable configurations, but also which are more appropriate according to their location within the terrain.

Focusing solely on the relationship between LST and GIT is not representative the complex interaction between cold and heat islands. Ventilation per se and fresh air exchange through circulation are important for heat stress relaxation. Nevertheless, the use of GITs in urban planning, as a quick screening method to roughly predict the thermal behaviour of existing and planned structures, can contribute to the design and simultaneous assessment of interventions. This is particularly relevant when competition for space leads to the necessity to control the efficiency and sufficiency of GCC adaption plans.

Acknowledgements

Thanks to BMBF for funding this research as part of INTERESS-I project under FKZ 01LR1705A1 and to Stadt Stuttgart for providing data. Kristen Jakstis did a great job in proof reading and improvements of written text.

References

- ANIELLO, C., MORGAN, K., BUSBEY, A. & NEWLAND, L. (1995), Mapping micro-urban heat islands using LANDSAT TM and a GIS. *Computers & Geosciences*, 21 (8), 965-969.
- ASADI, A., AREFI, H. & FATHIPOOR H. (2020), Simulation of green roofs and their potential mitigating effects on the urban heat island using an artificial neural network: A case study in Austin, Texas. *Advances in Space Research*, 66 (8), 1846-1862.
- BARTESAGHI-KOC, C., OSMOND, P. & PETERS, A. (2019a), Mapping and classifying green infrastructure typologies for climate-related studies based on remote sensing data. *Urban Forestry & Urban Greening*, 37, 154-167.
- BARTESAGHI-KOC, C., OSMOND, P. & PETERS, A. (2019b), Spatio-temporal patterns in green infrastructure as driver of land surface temperature variability: The case of Sydney. *International Journal of Applied Earth Observation and Geoinformation*, 83, 101903.
- BARTESAGHI-KOC, C., OSMOND, P. & PETERS, A. (2020), Quantifying the seasonal cooling capacity of 'green infrastructure types' (GITs): An approach to assess and mitigate surface urban heat island in Sydney, Australia. *Landscape and Urban Planning*, 203, 103893.
- CADENASSO, M. L., PICKETT S. T. A. & SCHWARZ, K. (2007), Spatial heterogeneity in urban ecosystems: reconceptualising land cover and a framework for classification. *Frontiers in Ecology and the Environment*, 5 (2), 80-88.
- KAPLAN, G., AVDAN, U. & AVDAN, Z. Y. (2018), Urban Heat Island Analysis Using the Landsat 8 Satellite Data: A Case Study in Skopje, Macedonia. *Proceedings*, 2 (7), 358.
- LEHMANN, I., MATHEY, J., RÖBLER, S., BRÄUER, A. & GOLDBERG, V. (2014), Urban vegetation structure types as a methodological approach for identifying ecosystem services – Application to the analysis of micro-climatic effects. *Ecological Indicators*, 42, 58-72.
- MCGARIGAL, K. (2015), FRAGSTATS Help. <http://www.umass.edu/landeco/research/fragstats/documents/fragstats.help.4.2.pdf> (15.03.2023).
- MOHAMMED, A., KHAN, A. & SANTAMOURIS, M. (2022), Numerical evaluation of enhanced green infrastructures for mitigating urban heat in a desert urban setting. *Build. Simul.* <https://doi.org/10.1007/s12273-022-0940-x>.
- NGARAMBE, J., SANTAMOURIS, M. & YUN, G. Y. (2022), The Impact of Urban Warming on the Mortality of Vulnerable Populations in Seoul. *Sustainability*, 14 (20), 13452.

- PHELAN, P. E., KALOUSH, K., MINER, M., GOLDEN, J., PHELAN, B., SILVA, H. & TAYLOR, R. A. (2015), Urban heat island: mechanisms, implications, and possible remedies. *Annual Review of Environment and Resources*, 40, 285-307.
- PLATT, R. V. & RAPOZA, L. (2008), An Evaluation of an Object-Oriented Paradigm for Land Use/Land Cover Classification. *The Professional Geographer*, 60 (1), 87-100.
- RANAGALAGE, M., ESTOQUE, R. C. & MURAYAMA Y. (2017), An Urban Heat Island Study of the Colombo Metropolitan Area, Sri Lanka, Based on Landsat Data (1997-2017). *ISPRS International Journal of Geo-Information*, 6 (7), 189.
- SANTAMOURIS, M. (2015), Analysing the heat island magnitude and characteristics in one hundred Asian and Australian cities and regions. *Science of The Total Environment*, 512-513, 582-598.
- STEWART I. D. & OKE T. R. (2012), Local Climate Zones for Urban Temperature Studies. *Bulletin of the American Meteorological Society*, 93 (12), 1879-1900.
- USGS. (2022), Landsat 8-9 Collection 2 (C2) Level 2 Science Product (L2SP) Guide. EROS Sioux Falls, South Dakota.
- VOLK, R., RAMBHIA, M., NABER, E. & SCHULTMANN, F. (2022), UrbanResource Assessment, Management, and Planning Tools for Land, Ecosystems, Urban Climate, Water, and Materials – A Review. *Sustainability* 2022, 14, 7203. [https:// doi.org/10.3390/su14127203](https://doi.org/10.3390/su14127203).
- ZAIN, A. F., PERMATASARI, P. A., AINY, C. N., DESTRIANA, N., MULYATI, D. F. & EDI, S. (2015), The detection of urban open space at Jakarta, Bogor, Depok, and Yangerang – Indonesia by using remote sensingtechnique for urban ecology analysis. *Procedia Environmental Sciences*, 24, 87-94.
- ZHOU, W., HUANG, G. & CADENASSO, M. L. (2011), Does spatial configuration matter? Understanding the effects of land cover pattern on land surface temperature in urban landscapes. *Landscape and urban planning*, 102 (1), 54-63.